

## OPTIMIZATION OF RIVER BANK PROTECTION DESIGN BY DISCRETE ELEMENT METHOD

**Adrian Priceputu**

**Adrian Liviu Bugea**

**Cosmin Victor Roșu**

**Manole Stelian Șerbulea**

Technical University of Civil Engineering Bucharest, **Romania**

### ABSTRACT

The river bank protection options are limited, in general, due to the ground conditions of the river bank and the necessity of limiting the stream velocity. The classical approach of using rip rap, and filling the river bank landscape up to the designed geometry is subjected to the random conditions of dropping and settlement of the boulders. In this case, the design, considering especially the quantitative estimation of the material needed, is based only on the designer's experience.

The paper aims to propose an up-to-date method of designing the rip rap, in order to reduce the stochastic impact of the technology and in situ conditions. The work is based on a forensic investigation of a real case study, which involved the local reconstruction of the Danube river bank by means of rip rap. The goal is attained by determining, using Monte Carlo simulations, the most probable rip rap configuration, through DEM (discrete element method) simulations. Furthermore, a validation process is carried out, based on the obtained results (number and size distribution of the boulders forming the rip rap), using coupled FEM-DEM analysis.

The DEM Monte Carlo simulations are performed using a non-commercial software created by the authors, part of a research still in progress, while the coupled FEM-DEM computations used for validation purposes are ran using Abaqus software. The paper also shows strengths and weaknesses of both used methods and software, while providing some guidelines for future similar works.

**Keywords:** riprap, discrete element method, numerical modelling, Monte Carlo analysis

### INTRODUCTION

Riprap revetment are an easy means of protecting riverbanks against erosion and provide several advantages such as low costs and easy installation. Several factors are subject to design, such as stone size, shape, weight, layer thickness, toe protection and filter capabilities. Generally, the design methods are based on empirical relations and estimating the necessary quantity of material is often difficult, as was found in a recent case study that followed a river bank landslide on the shore of the Danube River (fig. 1). The current paper presents a stochastic approach of using discrete element modelling to estimate the necessary quantity of riprap needed not only for the protection from erosion, but also to prevent further loss of stability.



Fig. 1: Area affected by landslide and related damage

## DEM MODEL

### Introduction

The discrete element method (DEM) is a numerical technique for describing the behaviour of discontinuous media, introduced by Cundall [1] in 1971. The modelled material is composed of independent individual elements, of any given shape, with any degree of freedom. The behaviour of the material is given by the interactions between individual particles that compose it. Several contact models have been proposed to describe the particles interactions, but generally, as described in fig. 2, contacts may be characterized by stiffness and damping, both on normal and tangential directions.

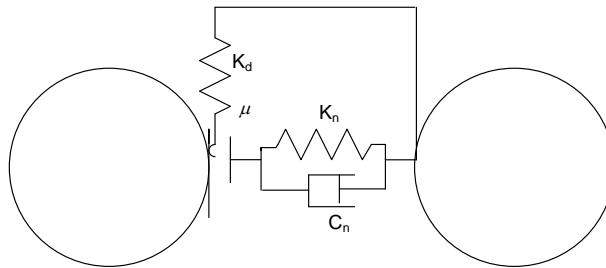


Fig. 2: General DEM contact model (after Oñate and Rojek [2])

The contact parameters may be constant (e.g. linear-spring-dashpot model, introduced by Cundall and Strack [3]) or may follow a law of variation (e.g. Hertzian-spring-dashpot, based on Hertz theory [4]). In terms of computation steps, the model alternates between applying the second law of Newton to assess particle accelerations while the contact forces are determined by means of a force-displacement law applied to a virtual overlapping of the particles that may occur in a time step. This is called the “soft-sphere” approach and was introduced by Cundall and Strack [3]. Another method would be the “hard-sphere” approach [5] which doesn’t allow particle superposition and cannot explicitly describe the contact forces. The DEM simulations presented in this paper were performed using a non-commercial software [6] that employs a soft-sphere approach using a linear-spring-dashpot model.

### Particle shapes

Usually, DEM software use spheres to describe particle shapes in 3D models, and discs in 2D models. Some authors have studied the effect of the particle shape and have developed ways to construct complex shape particles by forming rigid clusters of overlapping spheres [7]. The used software allows any 3D convex shape to be used as a dynamic particle, and any general 3D shape as a static element (e.g. terrain surface). The shapes used to describe the riprap were based on 3D rock models obtained from

scanned natural rock (fig. 3), which have been converted into convex hulls to allow dynamic behaviour. It is considered that the convex approximations of the rocks are less impactful on the behaviour of the material than using sphere particles or other simple shapes, although a comparison between the two approaches has not been performed.



Fig. 3: Shapes used to create riprap particles (3D models from free online source [8])

### Model parameters

The used software attaches a material to each element, which is described by friction and damping. The damping coefficient describes how much energy is lost at contact and may vary between 0 and 1. The models we developed employ a damping coefficient of 1, which renders a minimum bouncing effect on contacts.

Choosing the friction coefficient was more difficult, since there were no available mechanical tests to describe the internal friction of the material. Therefore, an inverse approach was considered. According to fig. 4, the angle of repose of dumped riprap depends on the mean grain size ( $d_{50}$ ) and the shape of the particles. Since the rocks used in our simulation have an average mass of 600kg, it can be found that their equivalent mean diameter is about 750mm (shown in the riprap revetment model section), thus expecting an angle of repose of about  $42^\circ \div 43^\circ$ . Thus a series of numerical tests were performed, with various material friction angles, to establish a relation between the two.

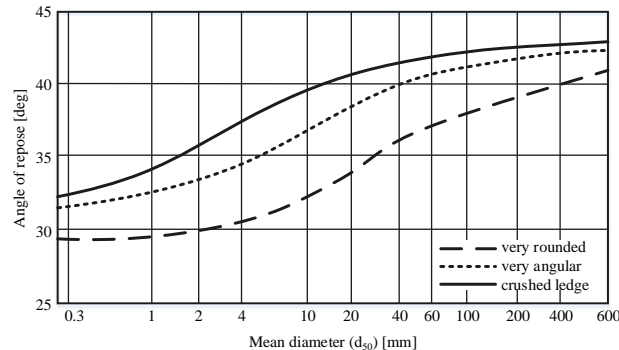


Fig. 4: Angle of repose of dumped riprap (after Simons and Senturk [9])

Although in theory, the angle of repose of a dry granular material is equal to the internal friction angle, as found by Lambe and Whitman [10] using an infinite slope stability analysis, previous studies have shown that the angle of repose is depending on several other factors. As Chik and Vallejo [11] have shown, the roughness of the base (the friction between the granular material and the base) has a significant impact. If the base is not rough enough, the material will suffer a spreading type of failure, leading to smaller angles of the slope. Discrete [12] and continuum [13] media simulations were performed on vertical cliff collapse problems, yielding angle of repose of  $10^\circ$  or less, for materials with internal friction angles of  $20^\circ$  or more. Furthermore, the shape of the particles was found to have an influence on the final angle of the slope, as shown by Jin et al. [14], reporting angles formed by tetrahedral particles about 20% larger than those of spherical particles.

Based on Jin et al. [14] reports, a 3D hopper was created for the angle of repose analysis, with a closed geometry and a funnel at the bottom, as shown in fig. 5. The hopper is made of frictionless material and serves as a vessel for disposing riprap to rest on a flat plate. A material with the same friction as the riprap is assigned to the plate in order to prevent lateral spreading effects due to low friction on the base.

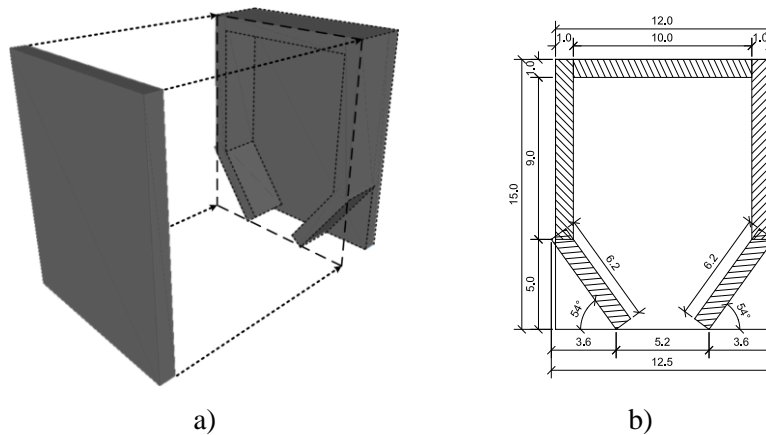


Fig. 5: Hopper geometry: a) isometric view; b) cross-section – dimensions in meters

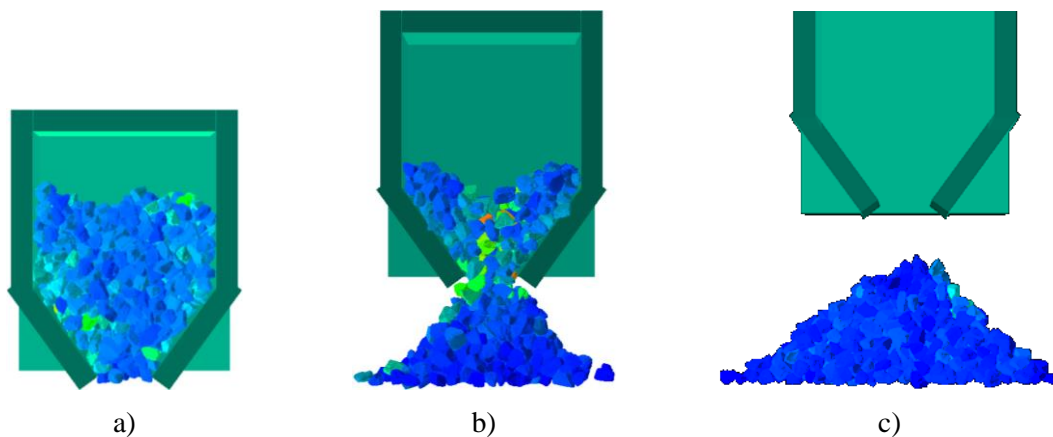


Fig. 6: Steps in performing the angle of repose analysis: a) generating the particles inside the hopper; b) discharging by moving the hopper upwards; c) final stage

A series of tests were performed, with particles having the same sizes and shapes as the riprap model, but various friction coefficients. The steps of the analysis, as graphically described in fig. 6, consist of first dispatching 500 riprap particles inside the hopper (a), than slowly lifting the hopper to allow the riprap to settle on the bottom plate (b). At the end of each stage (c), the positions of the particles are recorded and the test is restarted.

Since it was noticed that there is a slight variation in the results for a given friction angle, 10 analyses were performed for a constant friction angle, each of them yielding two angles of repose – at the left and the right side of the heap. The results were plotted (fig. 7) and a non-linear regression function was constructed, based on the Morgan-Mercer-Flodin (MMF) model, to express the variation between the friction angle and the angle of repose. The expression of the MMF model is given by equation 1 and the parameters obtained for the model were  $a=0.337$ ,  $b=7.003$ ,  $c=49.929$  and  $d=0.891$ . The coefficient of determination obtained for the MMF model was  $R^2=0.91$ . Based on the

obtained results, the friction angle for the riprap models was chosen  $\phi=63^\circ$  ( $\mu=1.96$ ) from the intersection of the MMF model with the  $42.5^\circ$  angle of repose line.

$$y(x) = \frac{a \cdot b + c \cdot x^d}{b + x^d} \quad (1)$$

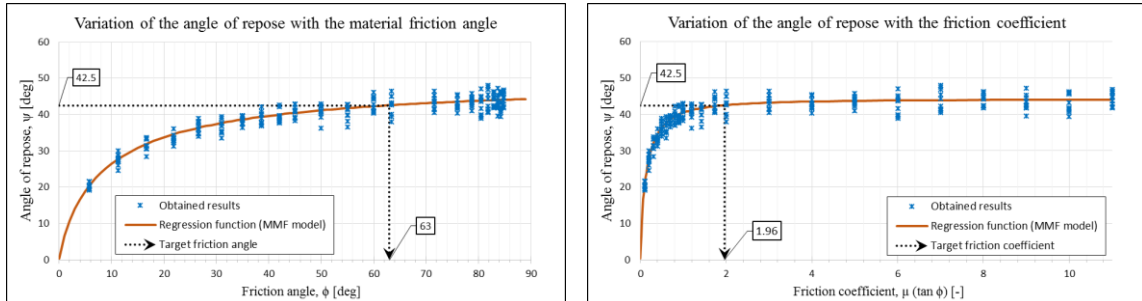


Fig. 7: Results of the angle of repose analysis

### Riprap revetment model

Based on the site topology, a typical cross-section was created, 120.0m long and 35.0m tall, and was loaded into the software to reproduce the site topology. For simplicity, the effect of the water was not taken into account within the model, but we consider that the positioning of the riprap, which is of main interest here, would not be greatly influenced by water-solid interaction. Due to the relatively large dimensions of the riprap (between 600mm and almost 900mm equivalent radius) the thickness of the cross-section had to be larger than 1.0m, but small enough to keep the necessary particle number relatively low. Therefore, the cross-section thickness was chosen to be 6.0m.

The used riprap particles have masses between 400kg and 800kg, as supplied by the practical project. Using equivalent diameters of each particle, which were computed assuming spheres with equal mass, the grain size distribution of the riprap was obtained as presented in fig. 8. The grain size distribution shown below was obtained using over 350'000 used in the simulations. The mean equivalent diameter ( $d_{50}$ ) is determined to be approximately 743mm, which according to Simons and Senturk [9] would produce an angle of repose of about  $42^\circ \div 43^\circ$ .

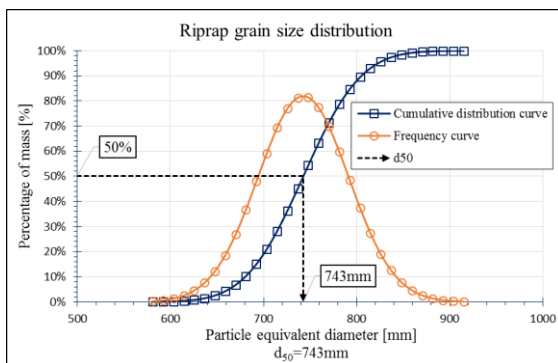


Fig. 8: Riprap grain size distribution

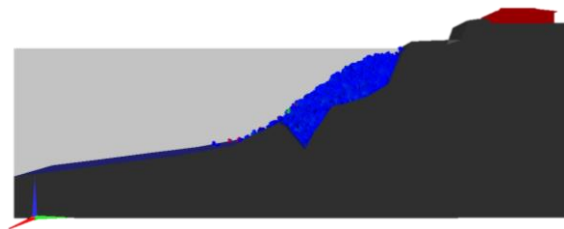


Fig. 9: Typical result after a simulation

A series of simulations were performed, by dropping a fixed number of particles on the cross-section and recording the positions of the particles at the end of the simulation (a typical result at the end of a simulation with 2000 particles is shown in fig. 9). A set of 250 simulations were performed with 600, 800, 1000, 1200 and 1400, while 100

simulations were performed with 1600, 1800, 2000, 2200, 2400 and 2600 particles. The particles' shapes, sizes and starting positions are random at each start of the simulation, using a pseudo-random number generation function, thus the end result is different for each simulation.

**Results**

The cross-section is divided longitudinally into segments of 1.0m, on which both the free-surface of the riprap revetment and the gravitational forces are computed. For every set of analyses regarding a fixed number of particles, a normal distribution of the particles was assumed in every point along the profile. Therefore, the probability of particles distribution can be assessed. Fig. 10 shows a sample of the obtained data, with the distribution of vertical forces along the profile, for 5% 50% (mean values) and 95% exceedance probabilities, while fig. 11 shows the corresponding standard deviations along the profile.

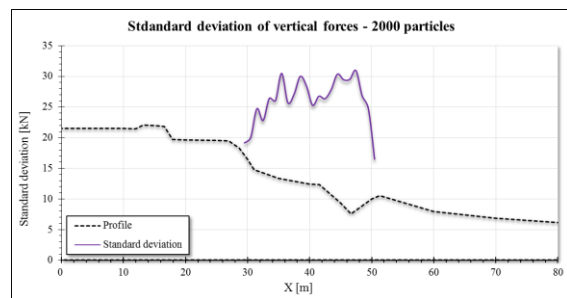
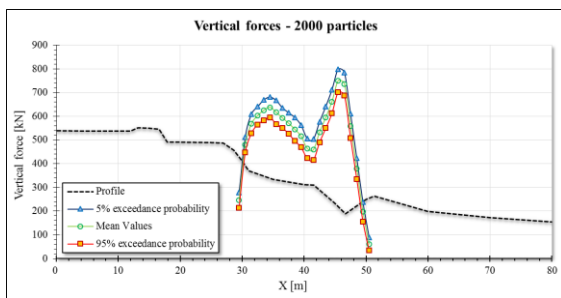


Fig. 10: Vertical forces distribution along the profile for 2000 particles

Fig. 11: Standard deviation distribution of the vertical forces for 2000 particles

By grouping the distributions resulted for each set of analyses, one can obtain a measurement of the variation of vertical forces and particles distribution along the profile, with increasing number of particles. Fig. 12 and 13 show mean values of positions and vertical forces obtained for all the analyses, but any amount of probability can be used to produce the results.

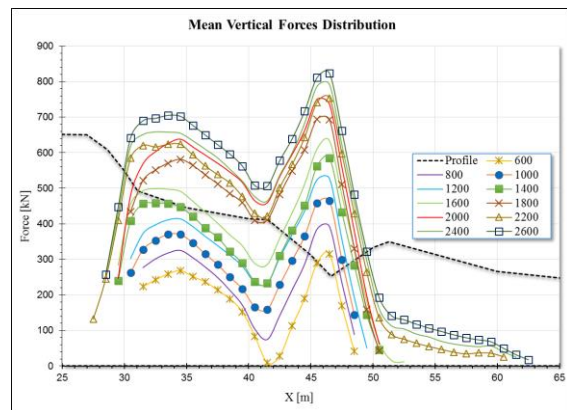
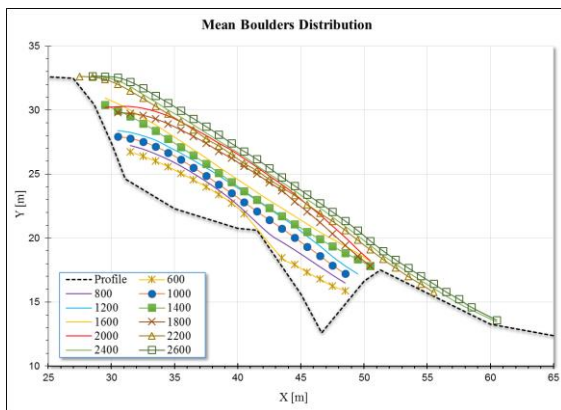


Fig. 12: Mean position of the free surfaces obtained for each set of simulations

Fig. 13: Mean vertical forces distribution for each set of simulations

**FEM MODEL**

A coupled FEM-DEM model was constructed to test one of the obtained DEM results (the 2000 particles model). The model was developed in Abaqus [15], which enables the



interaction between DEM and FEM elements. The simulation is based on a two stage computation: the first stage (static solver) is computed in order to induce the initial stress-strain state of the soil, while the second (dynamic explicit), is laying the discrete particles onto their approximately known equilibrium positions. The interaction, boundary and loading conditions have respected the ones considered during the DEM simulations.

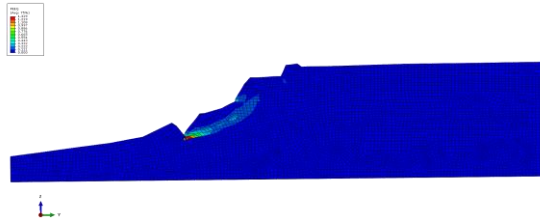


Fig. 14: Plastic shear strains after the consolidation stage

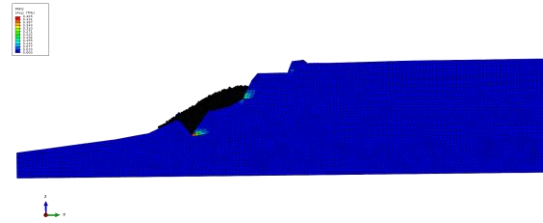


Fig. 15: Plastic shear strains after the riprap layout

Among the obtained results, after resetting the displacements, there can be observed that an overall backward movement appeared, as the riprap is pushing against the slope (maximum displacement 32.5cm, fig. 16, of which 17.6cm on the horizontal direction).

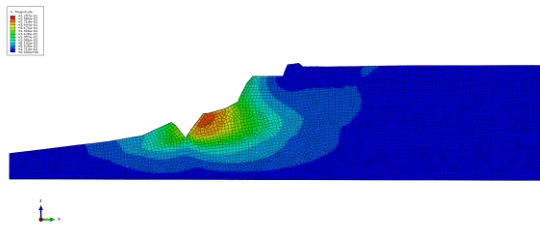


Fig. 16: Overall displacements after riprap

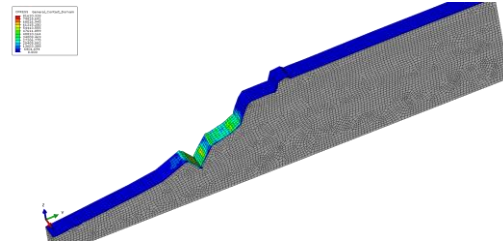


Fig. 17: Riprap contact pressures on the soil

The contact pressures, as a direct link to the initial DEM model, provided values between 6.8 and 81.62kPa, similar to the ones determined by means of discretization of the vertical forces already computed. There is still a slight difference between the two, as the later ones provide information of contact normal to the soil shape, and not only on vertical direction.

The maximum obtained slope using the coupled FEM-DEM model is about  $30.42^\circ$ , while an overall value lowers to  $27.69^\circ$ , due to soil's high compressibility.

## CONCLUSIONS

The presented work describes a methodology that is able to simulate the stochastic behaviour of riprap dumping. Starting from the parameters that can be determined through classical design, based mostly on empirical relations and nomograms, the presented approach can take the design further and assess a probability of distribution of the riprap for various quantities of material. The obtained results can be used to more accurately predict the costs of construction, and moreover, to determine the probability of obtaining a stable slope. The method does not supply a ready to use manual for riprap revetment design, but rather provides a means of quantifying the reliability of obtaining the design conditions. Although the used DEM software is not able to provide a safety factor variation of the models, the results can be used to create a coupled FEM-DEM analysis, as was shown, or even a simple LEM model to assess the stability of the

obtained configuration. However, the set of stochastic analyses shown could not have been performed in classical software.

## REFERENCES

- [1] Cundall P.A. A computer model for simulating progressive, large-scale movements in blocky rock systems. Proceedings of Symposium of International Society of Rock Mechanics, Nancy, France, vol. 2, pp. 129-136, 1971;
- [2] Oñate E. & Rojek J. Combination of discrete element and finite element methods for dynamic analysis of geomechanics problems, Computer Methods in Applied Mechanics and Engineering 193, pp. 3087-3128, 2004;
- [3] Cundall P.A. & Strack O.D.L. A discrete numerical model for granular assemblies, Geotechnique, vol. 29, no. 1, pp. 47-65, 1979;
- [4] Hertz H., Über die berührung fester elastischer körper, Journal für die Reine und Angewandte Mathematik, vol. 92, pp. 156-171, 1882;
- [5] Hoomans B.P.B., Kuipers J.A.M., Briels W.J. & Van Swaaij W.P.M. Discrete particle simulation of bubble and slug formation in a two-dimensional gas-fluidized bed: A hard-sphere approach, Chemical Engineering Science, vol. 51, no. 1, pp. 99-108, 1996;
- [6] Priceputu A. Discrete element method software application for cohesionless soil models, Proceedings of the 5th International Young Geotechnical Engineers' Conference, vol. 2, pp. 273- 276, 2013;
- [7] Lu M. & McDowell G.R. The importance of modelling ballast particle shape in the discrete element method, Granular Matter, vol. 9, pp. 69-80, 2007;
- [8] 3D Warehouse (March 2014). Retrieved from <https://3dwarehouse.sketchup.com/> courtesy of Intresto Rocksolver (<http://www.intresto.com.au/>);
- [9] Simons D.B. & Senturk F. Sediment Transport Technology, Water Resources Publications, Fort Collins, Colorado, 1977;
- [10] Lambe T.W. & Whitman R.V. Soil Mechanics, SI version. Wiley, New York, 1979;
- [11] Chik Z. & Vallejo L.E. Characterization of the angle of repose of binary granular materials, Canadian Geotechnical Journal 42, pp. 683-692, 2005;
- [12] Lacaze L. & Kerswell R.R. Axisymmetric granular collapse: a transient 3D flow test of viscoplasticity, Physical Review Letters 102, 108305, 2009;
- [13] Bui H.H., Fukagawa R., Sako K. & Ohno S. Lagrangian meshfree particles method (SPH) for large deformation and failure flows of geomaterial using elastic-plastic soil constitutive model, International Journal for Numerical and Analytical Methods 32, pp. 1537-1570, 2008;
- [14] Jin F., Xin H., Zhang C. & Sun Q. Probability-based contact algorithm for non-spherical particles in DEM, Powder Technology 212, pp. 134-144, 2011;
- [15] Abaqus/CAE 6.13, Dassault Systèmes, Providence, RI, USA, 2013.